

## RESEARCH ARTICLE

View Article Online

View Journal | View Issue

Cite this: *Inorg. Chem. Front.*, 2021, **8**, 4052A bifunctional robust metal sulfide with highly selective capture of Pb<sup>2+</sup> ions and luminescence sensing ability for heavy metals in aqueous media†Anastasia D. Pournara,<sup>a</sup> Christina-Georgia Bika,<sup>a</sup> Xitong Chen,<sup>b</sup> Theodore Lazarides,<sup>c</sup> Spyridon Kaziannis,<sup>d</sup> Pingyun Feng,<sup>b</sup> and Manolis J. Manos<sup>\*,a,e</sup>

Heavy metal ions represent hazardous and harmful contaminants for living organisms and the environment and thus, it is of urgent need to develop new materials sufficient to detect and remove them efficiently. Herein, we report the metal sulfide ion exchanger (MSIE) H<sub>x</sub>Ga<sub>x</sub>Ge<sub>4-x</sub>S<sub>8</sub>·yH<sub>2</sub>O (protonated UCR-20, **p-UCR-20**) which demonstrates exceptional capability for both detection and removal of heavy metals from aqueous samples. This material exhibited exceptional fast sorption kinetics (≤1 min), high sorption capacity (~527 mg g<sup>-1</sup>) and remarkable selectivity for Pb<sup>2+</sup> towards various common alkali and alkaline earth cations and in highly acidic to alkaline conditions. Even more importantly, **p-UCR-20** in its composite form with calcium alginate was used as stationary phase (along with silica sand) in a fixed-bed ion exchange column and was found capable of eliminating traces of Pb<sup>2+</sup> from a large volume of a wastewater simulant solution. Photophysical studies revealed that **p-UCR-20** shows excellent luminescence sensing properties for Pb<sup>2+</sup>, achieving limits of detection below the acceptable Pb levels in water and such efficient sensing properties are largely retained even in the presence of several antagonistic species in large excess. In addition, **p-UCR-20** displays highly efficient sensing properties for additional heavy metal ions, such as Ni<sup>2+</sup> and Cd<sup>2+</sup>. Overall, the results derived from the current study reveal for the first time that MSIES may be a source not only of excellent sorbents but also exceptional luminescent sensors for heavy metal ions in aqueous media.

Received 25th May 2021,  
Accepted 28th July 2021  
DOI: 10.1039/d1qi00666e

rsc.li/frontiers-inorganic

## Introduction

Access to clean freshwater represents a key challenge for the upcoming decades; therefore, the treatment of wastewater is currently widely investigated to compensate for dwindling water supplies, as it is a reliable alternative water source. The presence of heavy metals in aqueous ecosystems poses a major threat, due to their high toxicity, non-biodegradability, discharge and accumulation in living beings.<sup>1–5</sup> This issue is ever-increasing in less developed countries where many industrial

residues containing toxic heavy metals are often released into the environment without suitable purification, due to the lack of proper regulations and the high cost of the treatment technologies. Lead (Pb), owing to its physical properties including high strength, high pliability and low melting point, is one of the most desirable industrial raw material. Lead is still being used in battery manufacturing, metal plating, painting, ceramic and glass industries printing, and mining activities.<sup>6</sup> At the same time, Pb is considered as a very common and harmful element found in the environment, causing several undesired outcomes to brain, bones, kidneys, blood and also to cardiovascular, nervous and reproductive system.<sup>7</sup> The World Health Organization – WHO and the European Environmental Agency-EEA have set the maximum contaminant limit for Pb to 10 ppb, with the US Environmental Protection Agency-US EPA proposing a limit value of 15 ppb, while the maximum contaminant level goal is zero.<sup>8</sup> Since the use of Pb is still inevitable for the industrial activities, the efficient removal of Pb<sup>2+</sup> ions from aqueous environment is of great importance. In the direction of achieving the zero limit, several state-of-the-art methods and materials have been uti-

<sup>a</sup>Laboratory of Inorganic Chemistry, Department of Chemistry, University of Ioannina, 45110 Ioannina, Greece. E-mail: emanos@uoi.gr<sup>b</sup>Department of Chemistry, University of California, Riverside, CA 92521, USA<sup>c</sup>Laboratory of Inorganic Chemistry, Department of Chemistry, Aristotle University of Thessaloniki, 54124 Thessaloniki, Greece<sup>d</sup>Department of Physics, University of Ioannina, 45110 Ioannina, Greece<sup>e</sup>Institute of Materials Science and Computing, University Research Center of Ioannina, Ioannina, 45110, Greece

†Electronic supplementary information (ESI) available: Details of fluorescence experiments, determination of LODs, Stern–Volmer plots, EDS-elemental mapping. See DOI: 10.1039/d1qi00666e



lized for the removal of  $\text{Pb}^{2+}$  species from contaminated water. These methods include sorption,<sup>9,10</sup> ion exchange,<sup>11–13</sup> chemical precipitation,<sup>14,15</sup> membrane filtration,<sup>16</sup> and coagulation-flocculation.<sup>17</sup> Among them, sorption and ion exchange are simply operated, efficient and economic methods. Sulfur-containing materials represent attractive  $\text{Pb}^{2+}$  sorbents, considering that  $\text{Pb}^{2+}$ , as a soft acid, can form strong covalent bonds with soft  $\text{S}^{2-}$  groups. Metal sulfide ion exchangers (MSIEs) are the leaders of this category, as they own soft  $\text{S}^{2-}$  ligands and do not require additional functional groups into their frameworks.<sup>18</sup> So far, MSIEs with layered structures have been extensively studied for  $\text{Pb}^{2+}$  ion exchange, indicating excellent sorption capability.<sup>18,19</sup> In contrast, MSIEs with 3-D structures have been rarely studied for their heavy metal ion sorption properties.<sup>20</sup>

On the other hand, detection of heavy metal ions in water is also highly significant. Recent advances in optical technologies allow the design and construction of miniaturized, portable light detection devices. This fact, coupled with the ease and sensitivity with which light can be detected, has led to an increased interest in sensor systems based on luminescence.<sup>21–23</sup> Such sensors rely on the recording of changes in the emission signal of a luminescent material (often termed as *sensor element*) upon its, usually reversible, interaction with a targeted analyte. These analyte-induced changes in luminescence may subsequently be processed by an electronic system thereby allowing the analyte to be recognized and quantified. The most important property of a good sensory material is its ability to selectively bind a targeted species in such a way as to induce a perturbation in its electronic properties, which, in turn, leads to measurable changes in the material's emission signal. The most widely studied luminescent sensory materials are those based on small molecules bearing analyte-binding moieties<sup>24,25</sup> and porous fluorescent conjugated polymers.<sup>26</sup> Recently, there has been an increasing interest in luminescent metal-organic frameworks (LMOFs) for sensing applications as these materials combine permanent porosity, and therefore the ability to bind guest species, with luminescence properties.<sup>27–29</sup> Up to now, MSIE materials have not been investigated as sensors for heavy metals ions. This is not unexpected as only a handful of MSIEs are efficiently luminescent.

In an earlier study, Feng *et al.* reported a series of microporous and luminescent metal sulfides with the general formula  $(\text{Ga}_x\text{Ge}_{4-x}\text{S}_8)^{x-}$  (with the anionic charge of the framework balanced by the presence of organic ammonium cations), denoted as UCR-20.<sup>30</sup> The  $\text{K}^+$ -containing UCR-20 material has been recently studied for  $\text{Cs}^+$  ion exchange showing highly selective sorption capacity for this cation.<sup>31</sup> However, no heavy metal ion sorption nor luminescence sensing investigations have been reported for such materials, even though their porous structures with plenty of  $\text{S}^{2-}$  ligands make them particularly attractive for such investigations.

Herein we report the proton-containing version of UCR-20 material  $\text{H}_x\text{Ga}_x\text{Ge}_{4-x}\text{S}_8 \cdot y\text{H}_2\text{O}$  ( $x = 3.25$ ) (**p-UCR-20**). As a result of the replacement of bulky organic cations with the

labile  $\text{H}^+$ , **p-UCR-20** displayed an exceptional performance towards  $\text{Pb}^{2+}$  uptake from aqueous media with extremely rapid sorption kinetics ( $\leq 1$  min) and high sorption capacity ( $>500$  mg  $\text{g}^{-1}$ ). Importantly, **p-UCR-20**, in its composite form with alginate, was utilized in an ion exchange column and showed capability for quantitative removal of  $\text{Pb}^{2+}$  traces ( $\sim 100$  ppb) from large quantity of simulated wastewater. In addition, for the first time we demonstrate the highly efficient luminescence sensing properties of a metal sulfide ion exchanger. Thus, **p-UCR-20** was found particularly effective for the luminescence based-detection of heavy metal ions in concentrations well below their acceptable levels in water, even in the presence of various competitive cationic species. These results indicate that MSIEs may constitute not only efficient sorbents, but also promising luminescent sensors for heavy metal ions.

## Experimental section

### Materials

All reagents and solvents were commercially available and used as received.

**Synthesis of p-UCR-20.** The synthesis UCR-20GaGeS-AEP has been done as reported in literature.<sup>30</sup> The synthesis of **p-UCR-20** was achieved *via* treatment of UCR-20 with HCl acid. 20 mg (0.023 mmol) of UCR-20 are immersed into an aqueous solution of HCl (pH  $\sim 2$ , 10 mL) and kept under stirring for 2 d. The brownish powder was isolated *via* centrifugation, rinsed several times with water and dried under vacuum. Yield: 19 mg.

**Synthesis of p-UCR-20/CA composite.** 20 mg of sodium alginate (SA) was dissolved in 40 mL of warm water. 96 mg (0.15 mmol) **p-UCR-20** was dispersed in 8 mL of the SA solution. To this suspension, 96 mg (0.87 mmol) of  $\text{CaCl}_2$  was added under continuous stirring. The composite **p-UCR-20-CA** was immediately precipitated, collected by centrifugation, washed with water and acetone and dried under vacuum. Yield: 89 mg.

**Characterization of p-UCR-20.** PXRD diffraction patterns were recorded on a Bruker D2 Phaser X-ray diffractometer ( $\text{CuK}\alpha$  radiation, wavelength = 1.54184 Å). IR spectra were recorded on KBr pellets in the 4000–400  $\text{cm}^{-1}$  range using a PerkinElmer Spectrum GX spectrometer. Thermogravimetric analyses (TGA) were performed on a PerkinElmer Diamond system. Thermal analysis was conducted from 30 to 600 °C in nitrogen atmosphere (100 mL  $\text{min}^{-1}$  flow rate) with a heating rate of 10 °C  $\text{min}^{-1}$ . Energy dispersive spectroscopy (EDS) analyses were performed on a JEOL JSM6390LV scanning electron microscope (SEM) equipped with an Oxford INCA PentaFET-x3 energy dispersive X-ray spectroscopy (EDS) detector. Data acquisition was performed with an accelerating voltage of 20 kV and 120 s accumulation time.

### Batch ion-exchange studies/ $\text{Pb}^{2+}$ ion-exchange experiments with p-UCR-20

**Preparation of the  $\text{Pb}^{2+}$ ,  $\text{Ni}^{2+}$ ,  $\text{Cd}^{2+}$ ,  $\text{Zn}^{2+}$  and  $\text{Cu}^{2+}$  solutions.** A standard  $\text{Pb}^{2+}$  aqueous solution ( $C = 1000$  ppm) was pre-



pared *via* dissolution of 159.8 mg of  $\text{Pb}(\text{NO}_3)_2$  in 100 ml distilled  $\text{H}_2\text{O}$ . Likewise, we prepared standard aqueous solutions of  $\text{Ni}^{2+}$ ,  $\text{Cd}^{2+}$ ,  $\text{Zn}^{2+}$  and  $\text{Cu}^{2+}$ , by using  $\text{NiCl}_2$ ,  $\text{Cd}(\text{NO}_3)_2$ ,  $\text{Zn}(\text{NO}_3)_2 \cdot 6\text{H}_2\text{O}$  and  $\text{Cu}(\text{NO}_3)_2 \cdot 3\text{H}_2\text{O}$ , respectively. Metal ions solutions of 1 ppm concentration were prepared *via* dilution of the standard metal ions solutions.

**Batch sorption kinetics.** For the determination of the sorption kinetics,  $\text{Pb}^{2+}$  ion-exchange experiments of various reaction times (1–20 min) have been performed. For each experiment, a 10 mL sample of  $\text{Pb}^{2+}$  solution (initial  $\text{Pb}^{2+}$  concentration = 1 ppm,  $\text{pH} = 7 \pm 0.02$ ) was added to each vial (containing 10 mg of **p-UCR-20**) and the mixtures were kept under magnetic stirring for the designated reaction times.

**Sorption isotherms.** The  $\text{Pb}^{2+}$  uptake from solutions of various concentrations (1–1000 ppm) was studied by the batch method at  $V:m \sim 1000 \text{ mL g}^{-1}$ , room temperature and 10 min contact. These data were used for the determination of  $\text{Pb}^{2+}$  sorption isotherms.

**Effect of pH.** The variable pH ion exchange experiments were also carried out with the batch method at  $V:m$  ratio  $\sim 1000 \text{ mL g}^{-1}$ , room temperature and 20 min contact (initial  $\text{Pb}^{2+}$  concentration = 1 ppm). The pH values were adjusted using HCl and NaOH aqueous solutions.

**Selectivity study.** The selectivity of **p-UCR-20** towards several common cations was investigated through individual and competitive ion-exchange experiments in distilled and natural spring water. The composition of natural spring water was the following: hardness: 257 ppm (as  $\text{CaCO}_3$ );  $\text{pH} = 7.4$ ; cations:  $\text{Ca}^{2+} = 100 \text{ ppm}$ ,  $\text{Na}^+ = 2.82 \text{ ppm}$ ,  $\text{Mg}^{2+} = 1.83 \text{ ppm}$ ,  $\text{K}^+ = 0.52 \text{ ppm}$ ,  $\text{NH}_4^+ < 0.013 \text{ ppm}$ ; anions:  $\text{HCO}_3^- = 281 \text{ ppm}$ ,  $\text{Cl}^- < 8.26 \text{ ppm}$ ,  $\text{SO}_4^{2-} = 12.9 \text{ ppm}$ ,  $\text{NO}_3^- = 8.65 \text{ ppm}$ ,  $\text{NO}_2^- < 0.06 \text{ ppm}$ . For the competitive experiments, a mixture of 1 ppm each of  $\text{Pb}^{2+}$ ,  $\text{Ni}^{2+}$ ,  $\text{Cd}^{2+}$ ,  $\text{Zn}^{2+}$  and  $\text{Cu}^{2+}$  was added to 10 ml water, containing 10 mg of **p-UCR-20**.

**Determination of metal content.** The suspensions from the various sorption reactions were filtrated and the resulting solutions were analysed for their  $\text{Pb}^{2+}$ ,  $\text{Ni}^{2+}$ ,  $\text{Cd}^{2+}$ ,  $\text{Zn}^{2+}$  and  $\text{Cu}^{2+}$  content with anodic stripping voltammetry, using Trace Metal Analyzer (797 VA Computrace, Metrohm AG Ltd, Switzerland). More specifically, a three-electrode system was used comprising Hanging Mercury Drop Electrode (HMDE) as working electrode, Platinum (Pt) as auxiliary electrode and  $\text{Ag}/\text{AgCl}/\text{KCl}$  ( $3 \text{ mol L}^{-1}$ ) as reference electrode. The analysis has been done following the protocols developed by Metrohm (<http://www.metrohm.com/en/applications/#>). Each sorption experiment has been done at least twice and the reported sorption data represent the average of sorption results from the different sorption experiments. The difference between the concentrations of metal ions determined for the different sorption experiments was  $< 2\%$ .

**$\text{Pb}^{2+}$  leaching studies.** The  $\text{Pb}^{2+}$  leaching tests were conducted in distilled water and groundwater simulant solution at room temperature and 24 h contact. 100 mg of the loaded material were immersed in 100 ml distilled water (test 1) and 100 ml groundwater simulant solution (test 2) and kept under stirring for 24 h. The suspensions from both tests were fil-

trated and the resulting solutions were analysed for their  $\text{Pb}^{2+}$  content with anodic stripping voltammetry, using Trace Metal Analyzer (797 VA Computrace, Metrohm AG Ltd, Switzerland).

**Preparation of the column.** The stationary phase of the column comprised a mixture of 50 mg of **p-UCR-20-CA** and 5 g of sand (50–70 mesh  $\text{SiO}_2$ , 0.7 cm ID column, height = 9 cm). The column sorption studies were carried out with a waste-water simulant solution containing: 3 mM  $\text{NaHCO}_3$ , 0.143 mM  $\text{NaNO}_3$ ,  $10^{-3} \text{ mM NaH}_2\text{PO}_4 \cdot \text{H}_2\text{O}$ ,  $5 \times 10^{-2} \text{ mM NaF}$ , 0.33 mM  $\text{Na}_2\text{SiO}_3 \cdot 5\text{H}_2\text{O}$ , 0.99 mM  $\text{CaCl}_2 \cdot 2\text{H}_2\text{O}$ , 5 mM  $\text{MgSO}_4 \cdot 7\text{H}_2\text{O}$ ,  $4.8 \times 10^{-4} \text{ mM Pb}^{2+}$ .<sup>32</sup> The pH of this solution was adjusted to  $7 \pm 0.02$ . Several bed volumes of the solution were passed through the column and the effluents collected at the bottom in glass vials and measured with anodic stripping voltammetry. The flow rate in the column sorption studies was  $1 \text{ mL min}^{-1}$ .

**Preparation of p-UCR-20 suspension for fluorescence titration measurements.** 5 mg (0.008 mmol) of **p-UCR-20** were dispersed in 5 mL  $\text{H}_2\text{O}$  containing 50 mg (0.14 mmol) of Cetyltrimethylammonium Bromide (CTAB) and stirred for 24 h. Part of the **p-UCR-20-CTAB** solution was further diluted roughly by ten times in distilled water. The concentration was tuned to achieve a  $\sim 10\%$  absorption at the wavelength of excitation corresponding to a 1 cm path length. A 5 ml portion of the final solution was placed in a  $1 \times 1 \times 5 \text{ cm}$  quartz cuvette for the fluorescence quenching experiments and it was magnetically stirred continuously during the measurements. Details for the experimental setup (Fig. S1, ESI†) and the procedure for the fluorescence titration measurements are given in ESI.†

## Results and discussion

### Synthesis

As we have already mentioned in the introduction, 3-D MSIE materials have been rarely applied in heavy metal ion exchange.<sup>15</sup> In addition, MSIEs in general have not been studied as luminescent sensors. Being motivated from this lack, we decided to investigate UCR-20, as a representative MSIE with a porous 3-D framework, for its ability not only to remove but also to determine a series of emergent contaminants. UCR-20 displays a 3-D four-connected network based on corner-sharing T2 ( $\text{M}_4\text{S}_{10}$ ) supertetrahedral units.<sup>30</sup> The large pores of UCR-20 are filled with bulky organic ammonium cations. Since we aimed in a material with fast sorption kinetics, we decided to replace the relatively large organic guests with proton ions, the smallest possible cationic species. To this end, we treated UCR-20 with an acidic aqueous solution ( $10^{-2} \text{ M HCl}$ ), resulting in the release of organic counterions and the insertion of proton species (Fig. 1). The isolated proton-containing material (**p-UCR-20**) was proved to be an excellent sorbent and highly efficient luminescence sensor for heavy metal ions, as it will be shown below.

### Characterization of p-UCR-20 and $\text{Pb}^{2+}$ -loaded materials

The PXRD pattern of **p-UCR-20** is very similar to that calculated from the crystal structure of UCR-20 (Fig. 2), indicating that





Fig. 1 Schematic representation of the synthesis of p-UCR-20 by protonation of UCR-20.



Fig. 2 PXRD patterns of UCR-20 (calculated) and p-UCR-20.

the structure of pristine material remained intact after the protonation process. The characteristic IR peaks of AEP between 2700–3000  $\text{cm}^{-1}$  are almost eliminated after protonation of UCR-20, which supports the near-complete replacement of  $\text{AEPH}_2^{2+}$  by  $\text{H}^+$  cations (Fig. 3). TGA data of p-UCR-20 revealed a sharp weight loss up to 120  $^{\circ}\text{C}$ , which is assigned to the release of water molecules (4.7 moles per formula unit). In contrast, pristine UCR-20 shows almost no weight loss in this temperature range, as its pores contain no water and are filled exclusively by  $\text{AEPH}_2^{2+}$  cations (Fig. 4).

The  $\text{Pb}^{2+}$ -exchanged material was characterized with SEM-EDS and PXRD. EDS data and mapping images confirmed the presence of  $\text{Pb}^{2+}$  in the loaded material (Fig. S2 and 3<sup>†</sup>). PXRD data (Fig. S4a<sup>†</sup>) revealed that the structure of p-UCR-20 is preserved when the material is treated with low  $\text{Pb}^{2+}$  concentrations (up to 1 ppm), whereas the crystallinity of the compound is deteriorated upon its treatment with highly concentrated (1000 ppm)  $\text{Pb}^{2+}$  solutions (Fig. S4b<sup>†</sup>).

### $\text{Pb}^{2+}$ exchange studies of the p-UCR-20

**Batch sorption kinetics.** The sorption investigations of the p-UCR-20 towards  $\text{Pb}^{2+}$  were initiated with the determination of sorption kinetics through variable time experiments from 1 to 20 min. Surprisingly, no residues of  $\text{Pb}^{2+}$  were detected at

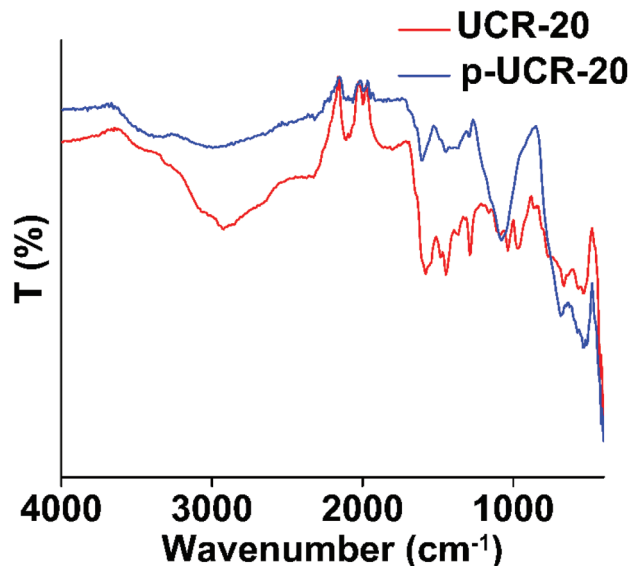


Fig. 3 FTIR spectra of UCR-20 and p-UCR-20.



Fig. 4 TGA data of UCR-20 and p-UCR-20.

the solutions, even with an extremely short (1 min) treatment of p-UCR-20 with the  $\text{Pb}^{2+}$  solution (initial concentration = 1 ppm,  $\text{pH} = 7 \pm 0.02$ ). It is worth mentioning that the detection limit of anodic stripping voltammetry, used for the determination of  $\text{Pb}^{2+}$ , is as low as 100 ppt. Consequently, p-UCR-20 displays extraordinary fast sorption kinetics, as it is capable to remove  $\geq 99.9999\%$  of the initial  $\text{Pb}^{2+}$  content within only 1 minute of contact.

Afterwards, we examined the sorption kinetics of the pristine UCR-20 under the same conditions. The pristine material displayed also rapid kinetics with 99.97% of the initial  $\text{Pb}^{2+}$  content been removed within only 1 minute, but the remaining  $\text{Pb}^{2+}$  content ( $\sim 30$  ppb) was higher than the acceptable limit for water (10–15 ppb). Even after 20 min of contact we were still able to detect  $\sim 2$  ppb of  $\text{Pb}^{2+}$  at the solution. The above data confirmed our initial hypothesis that the protonation will enhance the sorption kinetics of the UCR-20 material,





as a result of the inclusion of smaller size and more labile extra-framework cations (*i.e.*  $H^+$  ions). Note that hard  $H^+$  ions may interact weakly with the soft  $S^{2-}$  ions of the metal sulfide framework, thus being particularly amenable to be replaced by soft heavy metal ions.

**Sorption isotherms.** As a next step to our investigations, we performed concentration dependent experiments with **p-UCR-20** in aqueous solutions intentionally contaminated with  $Pb^{2+}$ . The fitting of sorption equilibrium data was performed with Langmuir, Freundlich and Langmuir–Freundlich equations (Fig. 5). The expressions of the three model equations are the following:<sup>18,33</sup>

$$(a) \text{ Langmuir } q = q_m \frac{bC_e}{1 + bC_e} \quad (1)$$

$$(b) \text{ Freundlich } q = K_F C_e^{\frac{1}{n}} \quad (2)$$

$$(c) \text{ Langmuir – Freundlich } q = q_m \frac{(bC_e)^n}{1 + (bC_e)^n} \quad (3)$$

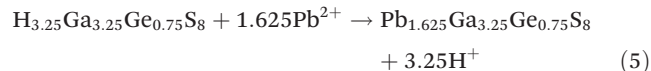
where  $q$  ( $mg\ g^{-1}$ ) is the amount of the cation sorbed at the equilibrium concentration  $C_e$  (ppm),  $q_m$  is the maximum sorption capacity of the sorbent,  $b$  ( $L\ mg^{-1}$ ) is the Langmuir constant related to the free energy of the sorption,  $K_F$  and  $n$  are the Freundlich constants.

The best fitting of the isotherm data of  $Pb^{2+}$  by the **p-UCR-20** was achieved by the Langmuir–Freundlich model.<sup>34</sup> The maximum sorption capacity was found to be  $527 \pm 30\ mg\ Pb^{2+}$  per g of **p-UCR-20**. Moreover, we performed equilibrium sorption experiments with the pristine UCR-20. The maximum sorption capacity for Pb was determined  $369 \pm 26\ mg\ Pb^{2+}$  per g of UCR-20. The experimental  $Pb^{2+}$  sorption capacities are close to the theoretical estimated capacities for the exchange of  $1.625\ AEPH_2^{2+}$  ( $351\ mg\ g^{-1}$ ) or  $3.25\ H^+$  cations ( $543\ mg\ g^{-1}$ ) by  $1.625\ Pb^{2+}$  cations.

The  $Pb^{2+}$  ion exchange processes for **UCR-20** and **p-UCR-20** are described by the following equations:



Fig. 5 Isotherm data for  $Pb^{2+}$  sorption by **p-UCR-20** and by **UCR-20**. The red lines represent the fitting of the data with the Langmuir–Freundlich model. Detailed fitting data are presented in Table S1.†



**Effect of pH.** The  $Pb^{2+}$  exchange studies for **p-UCR-20** were mainly carried out at  $pH = 7 \pm 0.02$ , to reproduce the conditions usually found in natural waters. However, the  $Pb^{2+}$  removal ability of **p-UCR-20** was also examined in additional pH values ranging from 0 to 10 (Fig. 6). Specifically, **p-UCR-20** retains high removal capability for  $Pb^{2+}$  in pH range from 1 to 10 ( $\pm 0.02$ ), with more than  $\sim 97\%$  of the initial  $Pb^{2+}$  content being removed. Surprisingly, the removal percentage in  $pH = 0$  was estimated to be  $\sim 40\%$  (initial Pb concentration = 1 ppm), indicating an exceptional sorbent even under extreme acidic conditions. This is attributed to the soft  $S^{2-}$  ligands of **p-UCR-20** framework showing weak interactions with the hard  $H^+$  ions.

**Effect of ionic strength-selectivity studies.** We have also investigated the effect of ionic strength on the  $Pb^{2+}$  sorption capability of **p-UCR-20**. To this end, we have studied  $Pb^{2+}$  sorption from natural spring water solutions artificially contaminated with  $Pb^{2+}$  (initial concentration = 1 ppm). Note that these solutions contained several alkaline and alkaline earth cations in relatively high concentrations and large excess (up to 500-fold) in relation to the Pb content (the composition of natural spring water samples is given in Experimental section). The results revealed that **p-UCR-20** was able to remove 99.4% of the initial  $Pb^{2+}$  amount from these samples, thus indicating no effect of the high ionic strength on  $Pb^{2+}$  sorption. In addition, we have examined the selectivity of **p-UCR-20** for  $Pb^{2+}$  over other heavy metal ions. Experiments were conducted in 10 ml distilled water containing a mixture of  $Pb^{2+}$ ,  $Ni^{2+}$ ,  $Cd^{2+}$ ,  $Zn^{2+}$  and  $Cu^{2+}$  (each with an initial concentration of 1 ppm) and 10 mg of **p-UCR-20**. The removal percentages were calculated to be 99.95%, 93%, 99.74%, 77% and 82.36% for  $Pb^{2+}$ ,  $Ni^{2+}$ ,  $Cd^{2+}$ ,  $Zn^{2+}$  and  $Cu^{2+}$ , respectively (Table 1). As a further step to our investigations, we repeated the above experiments using natural spring water samples intentionally contaminated by 1 ppm for each of the examined heavy metal ions, to simulate the real-world wastewater conditions. The results showed removal percentages of 99.4%, 95.5%, 99.7%, 76.1% and 84.5% for  $Pb^{2+}$ ,  $Ni^{2+}$ ,  $Cd^{2+}$ ,  $Zn^{2+}$  and  $Cu^{2+}$ , respect-



Fig. 6  $\% Pb^{2+}$  removal by **p-UCR-20** vs. pH.



**Table 1** Results of the ion exchange selectivity studies

Sample	$C_0$ (ppb)	$C_e$ (ppb)	% removal
Mixture of ions <sup>a</sup>	1000 <sup>c</sup>	0.5(Pb), 2.54(Cd), 67(Ni), 176(Cu), 230(Zn)	99.95(Pb), 99.74(Cd), 93(Ni), 82.36(Cu), 77(Zn)
Mixture of ions <sup>b</sup>	1000 <sup>c</sup>	6(Pb), 3(Cd), 45(Ni), 155(Cu), 239(Zn)	99.4(Pb), 99.7(Cd), 95.5(Ni), 84.5(Cu), 76.1 (Zn)

<sup>a</sup> Distilled water. <sup>b</sup> Natural spring water (its composition is provided in Experimental section). <sup>c</sup> Initial concentration of each ion.

ively (Table 1). The above results indicated **p-UCR-20** as an excellent sorbent for  $\text{Pb}^{2+}$  even in the presence of several competitive cations. Importantly, in all competitive sorption experiments, the final Pb concentrations were found well-below the acceptable Pb levels in water. In parallel, **p-UCR-20** was also highly efficient for removal of additional toxic metal ions such as  $\text{Cd}^{2+}$  and  $\text{Ni}^{2+}$ .

**Column ion exchange study.** The promising results obtained from batch ion exchange studies motivated us to explore the capability of **p-UCR-20** to uptake  $\text{Pb}^{2+}$  using fixed-bed ion exchange columns, which are usually employed in industrial wastewater processes. Note that MSIEs reported so far in literature have been rarely studied for heavy metal ion sorption under continuous flow conditions. In fact, as-prepared MSIEs cannot be used as stationary phase in ion exchange columns due to the small size of their particles (with a few exceptions)<sup>35,36</sup> and their tendency to form fine water suspensions.<sup>20,37</sup> Indeed, the material **p-UCR-20** is isolated as very light powder that forms fine suspensions in the water, thus flowing out of the prepared columns. To overcome this drawback and utilize **p-UCR-20** as a stationary phase, we transformed it into a composite material with calcium alginate (CA) which is not easily dispersed in water, since its particles are covered by CA shell.<sup>20,37,38</sup> The composite **p-UCR-20-CA** was prepared with only 4 wt% of CA. Thus, the alginate shell was not thick enough to prevent the diffusion of ions into the frameworks' pores and thus, the material retained its exceptional sorption kinetics.

As we have done in previous studies with alginate composites,<sup>20,37–39</sup> the stationary phase in the column consisted of the composite material **p-UCR-20-CA** and silica sand (**p-UCR-20-CA** : sand mass ratio = 1 : 100). The column study was conducted with a ground water simulant solution (its composition is given in the Experimental section) containing traces of  $\text{Pb}^{2+}$  (initial  $\text{Pb}^{2+}$  concentration = 100 ppb). Besides  $\text{Pb}^{2+}$  cations, the simulant solution contained a variety of competitive cations with concentrations up to  $10^4$  times higher than that of  $\text{Pb}^{2+}$ . The results indicated that 0.95 L of the solution passed through the column exhibited a concentration <10 ppb, *i.e.* below the allowed WHO and EU levels for  $\text{Pb}^{2+}$  in water (Fig. 7). Furthermore, no traces of  $\text{Pb}^{2+}$  were detected before ~0.6 L of simulant solution passed through the column. These results are particularly significant considering that (a) only 50 mg of the **p-UCR-20** were efficient to decontaminate almost 1 L of wastewater and (b) industrial wastewater treatment processes demand materials that can be utilized successfully in ion exchange columns.



**Fig. 7** Column sorption data with a wastewater simulant solution (flow rate  $\sim 1.0 \text{ mL min}^{-1}$ , one bed volume = 3.5 mL, stationary phase **p-UCR-20-CA**/sand = 0.05 g : 5 g, initial Pb concentration = 100 ppb).  $V_{\text{eff}}$  and  $C_{\text{eff}}$  represent the volume (mL) and  $\text{Pb}^{2+}$  concentration (ppb) of the solution passed through the column (*i.e.* effluent) respectively.

### Mechanism of $\text{Pb}^{2+}$ sorption by **p-UCR-20**

The results from the sorption studies indicate that the process proceeds *via* a rapid ion exchange between the labile  $\text{H}^+$  and  $\text{Pb}^{2+}$  species (see eqn (5)). The capture of  $\text{Pb}^{2+}$  by **p-UCR-20** is facilitated by the highly porous structure of this material and the presence of numerous  $\text{S}^{2-}$  ligands. The latter constitute binding sites for soft heavy metal ions such as  $\text{Pb}^{2+}$ , as revealed by several studies with MSIES.<sup>20</sup> In addition, the sorption of  $\text{Pb}^{2+}$  by **p-UCR-20** in either batch or continuous flow conditions is not affected by the presence of several cationic species such as  $\text{H}^+$ ,  $\text{Na}^+$ ,  $\text{Ca}^{2+}$ ,  $\text{Mg}^{2+}$  *etc.* This is attributed to the particularly weak interactions of hard cations with the soft sulfide-based framework of **p-UCR-20**. In contrast, the latter interacts particularly strongly with the soft  $\text{Pb}^{2+}$ , thus leading to the exceptional selectivity of **p-UCR-20** towards this cation.

### Comparison of **p-UCR-20** with other $\text{Pb}^{2+}$ sorbents

A comparison of the sorption capacities, as well as other important sorption properties, of various  $\text{Pb}^{2+}$  sorbents are provided in Table S2.† It can be seen that the maximum sorption capacity of **p-UCR-20** ( $527 \text{ mg g}^{-1}$ ) compares well with those of most efficient  $\text{Pb}^{2+}$  sorbents.<sup>40–42</sup> In addition, **p-UCR-20** represents the most effective  $\text{Pb}^{2+}$  sorbent among the metal sulfide ion exchangers, since it displays the fastest sorption kinetics (the equilibrium is reached within only 1 min) as



well the highest sorption capacity.<sup>18,43</sup> Furthermore, **p-UCR-20** is the only MSIE tested so far for the removal of  $\text{Pb}^{2+}$  under flow conditions, *i.e.* under conditions simulating the practical wastewater treatment.

### Reusability- $\text{Pb}^{2+}$ leaching studies

The regeneration of **p-UCR-20** after the  $\text{Pb}^{2+}$  sorption was investigated by treatment with dilute acidic solutions (0.01–0.1 M HCl); however, this process was not effective in removing Pb from the metal sulfide. Treatment with more concentrated acidic media (*e.g.*  $\geq 1$  M HCl) may result in the decomposition of the material. Thus, **p-UCR-20** is not reusable, as happens with almost all known MSIES.<sup>20</sup> This disadvantage, however, is compensated by the high sorption capacity of the material ( $>50\%$  heavy metal by weight). In addition, the strong binding of heavy metal ion into the UCR-20 framework and the no detectable  $\text{Pb}^{2+}$  leaching upon treatment of the loaded material with either distilled water or groundwater simulant solution indicate that the  $\text{Pb}^{2+}$ -laden material could be considered as solid waste safe for disposal. In fact, not always regeneration of sorbents is desirable, as this results in large amounts of secondary waste. In contrast, solid waste occupies much less space and can be safely handled and stored if it shows negligible leaching of toxic species.

### Luminescence sensing properties

The excellent sorption properties of **p-UCR-20** towards  $\text{Pb}^{2+}$  ions coupled with its documented photoemission properties<sup>30</sup> prompted us to test the material as a luminescent sensor for  $\text{Pb}^{2+}$  ions. At this point, we should mention that as synthesized **p-UCR-20** could not form a stable suspension in water, which is a requirement for luminescence titration investigations. After testing various ionic surfactants and hydrophilic organic polymers, we have found that CTAB produces sufficiently stable **p-UCR-20** aqueous suspensions for our fluorescence titration investigations. In agreement with the results originally reported by Feng *et al.*,<sup>30</sup> irradiation of an aqueous suspension of **p-UCR-20** at 380 nm (see ESI† for experimental details) with a laser beam gives rise to a broad emission signal with maximum at *ca.* 470 nm. Time-resolved emission measurements revealed that the emission of **p-UCR-20** shows a single exponential decay with a time constant of  $4.1 \pm 0.3$  ns which falls well within the fluorescence range.

Titration of a stirred suspension of **p-UCR-20** with aliquots of a 1.0 ppm standard solution of  $\text{Pb}^{2+}$  ions in distilled water, results in the gradual quenching of the material's emission (Fig. 8). We observe stabilization of the emission signal at  $\text{Pb}^{2+}$  concentrations above *ca.* 25 ppb with the final emission intensity being about 60% of the initial emission signal. The plot of signal intensity *versus*  $\text{Pb}^{2+}$  concentration shows excellent linearity up to *ca.* 20 ppb ( $R^2 = 0.980$ ) with a slope of  $S = -0.0171 \pm 0.0006$  ppb<sup>-1</sup> which, combined with the standard deviation of  $\text{SD} = 0.012$  for the measurement of the luminescence signal, leads to limits of detection and quantification of 2.1 and 7.0 ppb respectively (Fig. S5 and Table S3†). These values illustrate the extremely high sensitivity of **p-UCR-20** towards  $\text{Pb}^{2+}$  as



**Fig. 8** The fluorescence titration ( $\lambda_{\text{exc}} = 380$  nm) of a stirred suspension of **p-UCR-20** in water ( $0.1 \text{ mg mL}^{-1}$ ) upon the addition of aliquots from a  $\text{Pb}^{2+}$  standard stock solution (concentration = 1000 ppb) in distilled water.

both the LOD and LOQ values are below the EEA and US EPA acceptable levels of  $\text{Pb}^{2+}$  in water (10 and 15 ppb respectively).<sup>8</sup>

To further assess the sensing performance of **p-UCR-20** towards  $\text{Pb}^{2+}$  in samples which contain relatively large concentrations of other, potentially inhibiting, metal ions we performed titration experiments with potable water (containing 78.7 ppm  $\text{Ca}^{2+}$ , 3.45 ppm  $\text{Mg}^{2+}$ , 3.3 ppm  $\text{Na}^+$ , 1.04 ppm  $\text{K}^+$ ) spiked with 1 ppm of  $\text{Pb}^{2+}$ . The results, shown in Fig. 9 indicate that the emission of **p-UCR-20** gradually quenches with a stabilization at *ca.* 60% of the intensity of the original signal

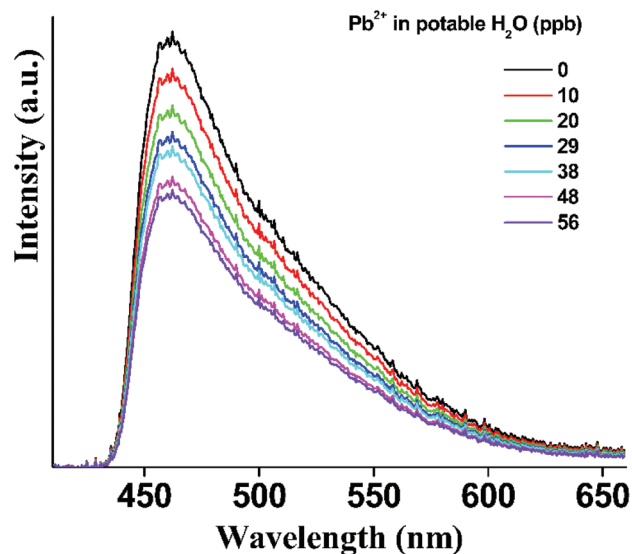


**Fig. 9** The fluorescence titration ( $\lambda_{\text{exc}} = 380$  nm) of a stirred suspension of **p-UCR-20** in water ( $0.1 \text{ mg mL}^{-1}$ ) upon the addition of aliquots from a  $\text{Pb}^{2+}$  standard stock solution (concentration = 1000 ppb) in potable water.



albeit with a considerably less steep slope compared to the case of the  $\text{Pb}^{2+}$  standard solution in distilled water. Nevertheless, the LOD and LOQ values being 6.4 and 21.2 ppb respectively are still comparable to the EU and USA acceptable levels of  $\text{Pb}^{2+}$  in water (*vide supra*) (Fig. S5†).

An analysis of the **p-UCR-20** emission quenching data in terms of the Stern–Volmer equation (eqn (4)) shows excellent linearity up to a  $\text{Pb}^{2+}$  concentration of *ca.* 0.12  $\mu\text{M}$  in both the cases of distilled and potable water ( $R^2 > 0.98$ ) with Stern–Volmer constants,  $K_{\text{SV}}$ , values of  $5.3 \times 10^6$  and  $2.0 \times 10^6 \text{ M}^{-1}$  respectively (Fig. S6†).

$$\frac{I_0}{I} = 1 + K_{\text{SV}}[\text{Pb}^{2+}]. \quad (4)$$

Additionally, we observed that the luminescence lifetime of **p-UCR-20** remains unchanged at all  $\text{Pb}^{2+}$  concentrations. These observations point towards one dominating quenching mechanism which, most possibly involves the entry of  $\text{Pb}^{2+}$  within the framework of **p-UCR-20**, which in turn causes static quenching of the material's emission possibly because the guest ions act as non-radiative exciton recombination centres.<sup>44</sup> This is in good agreement with the sorption data (*vide supra*) which demonstrated that  $\text{Pb}^{2+}$  ions enter the material's framework replacing the weakly bound protons most possibly driven by the favorable  $\text{S}^{2-} \cdots \text{Pb}^{2+}$  interactions. The markedly lower  $K_{\text{SV}}$  in the case of potable water suggests that the presence of hard metal ions in much larger concentrations can have an inhibitory effect on the interaction between **p-UCR-20** and  $\text{Pb}^{2+}$  which however remains strong.

Analogous sensing experiments were performed with  $\text{Cd}^{2+}$  and  $\text{Ni}^{2+}$  (Fig. S7–10†) which also show quenching of the emission of **p-UCR-20** albeit to a smaller extent. The results, in comparison to those of  $\text{Pb}^{2+}$ , are summarized in Table S3.†

It is worth emphasizing that with this study we demonstrate for the first time that a luminescent MSIE material can be attractive as a sensor as it combines the ability to selectively and efficiently sorb metal ions within its framework with a signal generating property.

## Conclusions

In summary, we have isolated **p-UCR-20**, a proton-containing MSIE with a 3-D open framework structure. This material was proved to be a first-rate  $\text{Pb}^{2+}$  sorbent, with extremely rapid sorption kinetics (equilibrium time  $\leq 1$  min) and excellent maximum sorption capacity (527  $\text{mg g}^{-1}$ ), comparable to the sorption capacities of the leading  $\text{Pb}^{2+}$  sorbent materials. Furthermore, **p-UCR-20** in its composite form with calcium alginate was utilized, in a mixture with sand, as stationary phase in an ion exchange column, which was found highly efficient for the removal of traces of  $\text{Pb}^{2+}$  from a large volume of wastewater simulant solution.

In addition to the sorption study, photophysical investigations set out in depth revealed that **p-UCR-20** represents also a very promising luminescent sensor, a property first time

demonstrated for MSIEs. The material was able to detect  $\text{Pb}^{2+}$  cations at concentrations quite lower than its safe upper limit in water, even in the presence of several competitive species in large excess. We should also note that **p-UCR-20** was effective to detect additional heavy metal cations, such as  $\text{Ni}^{2+}$  and  $\text{Cd}^{2+}$ . Overall, the results presented here, indicate the high efficiency of MSIEs not only for sorption but also for luminescence sensing of heavy metal ions, thus expanding the potential applications of these materials in environmental monitoring besides wastewater treatment.

## Author contributions

A. D. Pournara: investigation, formal analysis, writing-original draft, C-G. Bika: investigation, formal analysis, X. Chen: investigation, formal analysis, T. Lazarides: investigation, formal analysis, writing-review & editing, S. Kaziannis: investigation, formal analysis, writing-review & editing, Pingyun Feng: resources, formal analysis, writing-review & editing, M. J. Manos: conceptualization, supervision, resources, writing-original draft.

## Conflicts of interest

There are no conflicts to declare.

## Acknowledgements

We thank the Central Laser Facility at the University of Ioannina.

## References

- 1 R. Singh, N. Gautam, A. Mishra and R. Gupta, Heavy metals and living systems: An overview, *Indian J. Pharmacol.*, 2011, **43**, 246.
- 2 Z. Lin, Y. Hu, Y. Yuan, B. Hu and B. Wang, Comparative analysis of kinetics and mechanisms for  $\text{Pb}(\text{II})$  sorption onto three kinds of microplastics, *Ecotoxicol. Environ. Saf.*, 2021, **208**, 111451.
- 3 B. Hu, H. Wang, R. Liu and M. Qiu, Highly efficient U (VI) capture by amidoxime/carbon nitride composites, *Chemosphere*, 2021, **274**, 129743.
- 4 S. Li, L. Dong, Z. Wei, G. Sheng, K. Du and B. Hu, Adsorption and mechanistic study of the invasive plant-derived biochar functionalized with CaAl-LDH for Eu(III) in water, *J. Environ. Sci.*, 2020, **96**, 127–137.
- 5 S. Dai, N. Wang, C. Qi, X. Wang, Y. Ma, L. Yang, X. Liu, Q. Huang, C. Nie, B. Hu and X. Wang, Preparation of core-shell structure  $\text{Fe}_3\text{O}_4@\text{C}@\text{MnO}_2$  nanoparticles for efficient elimination of U (VI) and Eu(III) ions, *Sci. Total Environ.*, 2019, **685**, 986–996.





- 6 H. Sone, B. Fugetsu and S. Tanaka, Selective elimination of lead(II) ions by alginate/polyurethane composite foams, *J. Hazard. Mater.*, 2009, **162**, 423–429.
- 7 L. Järup, Hazards of heavy metal contamination, *Br. Med. Bull.*, 2003, **68**, 167–182.
- 8 E.P.A. US, National primary drinking water regulations: Long Term 1 Enhanced Surface Water Treatment Rule. Final rule, *Fed. Regist.*, 2002, **67**, 1811–1844.
- 9 J. Goel, K. Kadirvelu, C. Rajagopal and V. K. Garg, Removal of lead(II) by adsorption using treated granular activated carbon: Batch and column studies, *J. Hazard. Mater.*, 2005, **125**, 211–220.
- 10 X. Liu, H. Pang, X. Liu, Q. Li, N. Zhang, L. Mao, M. Qiu, B. Hu, H. Yang and X. Wang, Orderly porous covalent organic frameworks-based materials: superior adsorbents for pollutants removal from aqueous solutions, *The Innovation*, 2021, **2**, 100076.
- 11 A. Lalmi, K.-E. Bouhidel, B. Sahraoui and C. El H. Anfi, Removal of lead from polluted waters using ion exchange resin with  $\text{Ca}(\text{NO}_3)_2$  for elution, *Hydrometallurgy*, 2018, **178**, 287–293.
- 12 X. Cai, J. Li, Z. Zhang, F. Yang, R. Dong and L. Chen, Novel  $\text{Pb}^{2+}$  Ion Imprinted Polymers Based on Ionic Interaction via Synergy of Dual Functional Monomers for Selective Solid-Phase Extraction of  $\text{Pb}^{2+}$  in Water Samples, *ACS Appl. Mater. Interfaces*, 2014, **6**, 305–313.
- 13 L. Mi, H. Hou, Z. Song, H. Han and Y. Fan, Polymeric Zinc Ferrocenyl Sulfonate as a Molecular Aspirator for the Removal of Toxic Metal Ions, *Chem. – Eur. J.*, 2008, **14**, 1814–1821.
- 14 F. Fu, L. Xie, B. Tang, Q. Wang and S. Jiang, Application of a novel strategy—Advanced Fenton-chemical precipitation to the treatment of strong stability chelated heavy metal containing wastewater, *Chem. Eng. J.*, 2012, **189–190**, 283–287.
- 15 M. M. Matlock, B. S. Howerton and D. A. Atwood, Chemical Precipitation of Lead from Lead Battery Recycling Plant Wastewater, *Ind. Eng. Chem. Res.*, 2002, **41**, 1579–1582.
- 16 M. Soylak, Y. E. Unsal, N. Kizil and A. Aydin, Utilization of membrane filtration for preconcentration and determination of Cu(II) and Pb(II) in food, water and geological samples by atomic absorption spectrometry, *Food Chem. Toxicol.*, 2010, **48**, 517–521.
- 17 A. R. Karbassi and S. Nadjafpour, Flocculation of dissolved Pb, Cu, Zn and Mn during estuarine mixing of river water with the Caspian Sea, *Environ. Pollut.*, 1996, **93**, 257–260.
- 18 M. J. Manos and M. G. Kanatzidis, Sequestration of heavy metals from water with layered metal sulfides, *Chem. – Eur. J.*, 2009, **15**, 4779–4784.
- 19 J.-R. Li, X. Wang, B. Yuan, M.-L. Fu and H.-J. Cui, Robust removal of heavy metals from water by intercalation chalcogenide  $[\text{CH}_3\text{NH}_3]_{2x}\text{Mn}_x\text{Sn}_{3-x}\text{S}_6 \cdot 0.5\text{H}_2\text{O}$ , *Appl. Surf. Sci.*, 2014, **320**, 112–119.
- 20 M. J. Manos and M. G. Kanatzidis, Metal sulfide ion exchangers: Superior sorbents for the capture of toxic and nuclear waste-related metal ions, *Chem. Sci.*, 2016, **7**, 4804–4824.
- 21 R. Rigler, M. Orrit and T. Basché, Single molecule spectroscopy nobel conference lectures: Preface, *Springer Series in Chemical Physics*, 2001, vol. **67**.
- 22 B. Kuswandi, Nuriman, J. Huskens and W. Verboom, Optical sensing systems for microfluidic devices: A review, *Anal. Chim. Acta*, 2007, **601**, 141–155.
- 23 N. M. M. Pires, T. Dong, U. Hanke and N. Hoivik, Recent developments in optical detection technologies in lab-on-a-chip devices for biosensing applications, *Sensors*, 2008, **14**, 15458–15479.
- 24 A. P. De Silva, Luminescent photoinduced electron transfer (PET) molecules for sensing and logic operations, *J. Phys. Chem. Lett.*, 2011, **2**, 2865–2871.
- 25 J. K. Tusa and H. He, Critical care analyzer with fluorescent optical chemosensors for blood analytes, *J. Mater. Chem.*, 2005, **15**, 2640–2647.
- 26 T. M. Swager, Iptycenes in the design of high performance polymers, *Acc. Chem. Res.*, 2008, **41**, 1181–1189.
- 27 M. D. Allendorf, C. A. Bauer, R. K. Bhakta and R. J. T. Houk, Luminescent metal-organic frameworks, *Chem. Soc. Rev.*, 2009, **38**, 1330–1352.
- 28 L. Shi, N. Li, D. Wang, M. Fan, S. Zhang and Z. Gong, Environmental pollution analysis based on the luminescent metal organic frameworks: A review, *TrAC, Trends Anal. Chem.*, 2021, **134**, 116131.
- 29 S. A. Diamantis, A. Margariti, A. D. Pournara, G. S. Papaefstathiou, M. J. Manos and T. Lazarides, Luminescent metal-organic frameworks as chemical sensors: Common pitfalls and proposed best practices, *Inorg. Chem. Front.*, 2018, **5**, 1493–1511.
- 30 N. Zheng, X. Bu, B. Wang and P. Feng, Microporous and photoluminescent chalcogenide zeolite analogs, *Science*, 2002, **298**, 2366–2369.
- 31 H. Yang, M. Luo, L. Luo, H. Wang, D. Hu, J. Lin, X. Wang, Y. Wang, S. Wang, X. Bu, P. Feng and T. Wu, Highly Selective and Rapid Uptake of Radionuclide Cesium Based on Robust Zeolitic Chalcogenide via Stepwise Ion-Exchange Strategy, *Chem. Mater.*, 2016, **28**, 8774–8780.
- 32 F. Pinakidou, E. Kaprara, M. Katsikini, E. C. Paloura, K. Simeonidis and M. Mitrakas, Sn(II) oxy-hydroxides as potential adsorbents for Cr(VI)-uptake from drinking water: An X-ray absorption study, *Sci. Total Environ.*, 2016, **551–552**, 246–253.
- 33 M. J. Manos, N. Ding and M. G. Kanatzidis, Layered metal sulfides: Exceptionally selective agents for radioactive strontium removal, *Proc. Natl. Acad. Sci. U. S. A.*, 2008, **105**, 3696–3699.
- 34 G. P. Jeppu and T. P. Clement, A modified Langmuir-Freundlich isotherm model for simulating pH-dependent adsorption effects, *J. Contam. Hydrol.*, 2012, **129–130**, 46–53.
- 35 X.-H. Qi, K.-Z. Du, M.-L. Feng, J.-R. Li, C.-F. Du, B. Zhang and X.-Y. Huang, A two-dimensionally microporous thios-



- tannate with superior  $\text{Cs}^+$  and  $\text{Sr}^{2+}$  ion-exchange property, *J. Mater. Chem. A*, 2015, **3**, 5665–5673.
- 36 Y.-J. Gao, H.-Y. Sun, J.-L. Li, X.-H. Qi, K.-Z. Du, Y.-Y. Liao, X.-Y. Huang, M.-L. Feng and M. G. Kanatzidis, Selective Capture of  $\text{Ba}^{2+}$ ,  $\text{Ni}^{2+}$ , and  $\text{Co}_2^+$  by a Robust Layered Metal Sulfide, *Chem. Mater.*, 2020, **32**, 1957–1963.
  - 37 M. G. Kanatzidis, D. Sarma and M. Manos, Column material for the capture of heavy metal and precious metal ions, *U.S. Patent No* 10,549,270, 2020.
  - 38 S. Rapti, A. Pournara, D. Sarma, I. T. Papadas, G. S. Armatas, A. C. Tsipis, T. Lazarides, M. G. Kanatzidis and M. J. Manos, Selective capture of hexavalent chromium from an anion-exchange column of metal organic resin-alginic acid composite, *Chem. Sci.*, 2016, **7**, 2427–2436.
  - 39 S. Rapti, A. Pournara, D. Sarma, I. T. Papadas, G. S. Armatas, Y. S. Hassan, M. H. Alkordi, M. G. Kanatzidis and M. J. Manos, Rapid, green and inexpensive synthesis of high quality UiO-66 amino-functionalized materials with exceptional capability for removal of hexavalent chromium from industrial waste, *Inorg. Chem. Front.*, 2016, **3**, 635–644.
  - 40 A. D. Pournara, A. Margariti, G. D. Tarlas, A. Kourtellaris, V. Petkov, C. Kokkinos, A. Economou, G. S. Papaefstathiou and M. J. Manos, A  $\text{Ca}^{2+}$  MOF combining highly efficient sorption and capability for voltammetric determination of heavy metal ions in aqueous media, *J. Mater. Chem. A*, 2019, **7**, 15432–15443.
  - 41 N. Wang, X.-K. Ouyang, L.-Y. Yang and A. M. Omer, Fabrication of a Magnetic Cellulose Nanocrystal/Metal–Organic Framework Composite for Removal of  $\text{Pb(II)}$  from Water, *ACS Sustainable Chem. Eng.*, 2017, **5**, 10447–10458.
  - 42 C. Yu, X. Han, Z. Shao, L. Liu and H. Hou, High Efficiency and Fast Removal of Trace  $\text{Pb(II)}$  from Aqueous Solution by Carbomethoxy-Functionalized Metal–Organic Framework, *Cryst. Growth Des.*, 2018, **18**, 1474–1482.
  - 43 L. Ma, Q. Wang, S. M. Islam, Y. Liu, S. Ma and M. G. Kanatzidis, Highly Selective and Efficient Removal of Heavy Metals by Layered Double Hydroxide Intercalated with the  $\text{MoS}_4^{2-}$  Ion, *J. Am. Chem. Soc.*, 2016, **138**, 2858–2866.
  - 44 C. Xue, X. Fan, J. Zhang, D. Hu, X.-L. Wang, X. Wang, R. Zhou, H. Lin, Y. Li, D.-S. Li, X. Wei, D. Zheng, Y. Yang, K. Han and T. Wu, Direct observation of charge transfer between molecular heterojunctions based on inorganic semiconductor clusters, *Chem. Sci.*, 2020, **11**, 4085–4096.

